J Polym Environ (2008) 16:198–204
DOI 10.1007/s10924-008-0097-4

ORIGINAL PAPER

Preparation of Alginic Acid and Metal Alginate from Algae and their Comparative Study

Tara Sankar Pathak · Jin San Kim · Se-Jong Lee · Dae-Jin Baek · Ki-Jung Paeng

Published online: 3 May 2008

Abstract Alginic acid and metal alginates are prepared from fresh algae using extraction method. A FTIR spectrum indicates that alginic acid is converted into the metal alginate. Comparing calcium and cobalt alginates, asymmetric stretching of free carboxyl group of calcium alginate at 1630 cm^{-1} is shifted to 1585 cm^{-1} in cobalt alginate, due to the change of charge density, radius and atomic weight of the cation, creating a new environment around the carbonyl group. The strong exothermic peak of alginic acid in DSC thermogram indicates the decomposition of biopolymer, whereas strong exothermic peak of metal alginate in DSC thermogram attributed to the decomposition of biopolymer and formation of respective carbonate. Based on DSC study, the decomposition of cobalt alginate occurs at higher temperature comparing to those of sodium and calcium alginate, which may conclude into the higher stability of cobalt alginate. TGA results reveal that, cobalt alginate is more stable than calcium and sodium alginate at 300 °C temperature. Surface morphology (at same magnification), as well as porosity (%) and pore size distribution results change with metals present in different metal alginates.

T. S. Pathak · J. S. Kim · K.-J. Paeng (✉)
Department of Chemistry, Yonsei University, Wonju 220-710, South Korea
e-mail: paengk@yonsei.ac.kr

S.-J. Lee
Department of Materials Engineering, Kyungsung University, Busan 608-736, South Korea

D.-J. Baek
Department of Chemistry, Hanseo University, Seosan 352-820, South Korea

Keywords Alginates · Differential scanning calorimetry (DSC) · Porosity · Scanning electron microscopy (SEM) · Thermogravimetric analysis (TGA)

Introduction

Synthetic polymers such as ion-exchange resins and chelating resins have been widely used as effective adsorbents to collect radioactive nuclides, toxic metals, precious metals and base metals from aqueous solutions [1–3]. Naturally occurring biopolymers extracted from algae have been known to exhibit excellent adsorption ability for metal ions [4–6]. Alginic acid which occurs in brown seaweeds is a biopolymer carrying carboxyl groups capable of forming complexes with metal cations [7]. The ability of alginate to form gels by ion-exchange reaction with multivalent metal ions suggests its use as a metal adsorbent. Nicholas et al. [8] describes the physico-chemical properties of alginate gel beads. Many studies have addressed the collection of heavy metals such as Co, Cu, Cd and Zn by alginic acid [9–11]. Alginates are salts of alginic acid, which is a polyuronide made up of a sequence of two hexuronic acids: β-D mannuronic acid (M) and α-L guluronic acid (G) linked by a 1, 4 glycosidic bond that have extracted from all algae [12–19]. They exist as randomly arranged homogenous blocks (MM and GG) and heterogenous blocks (GM) along the polymer chains depending on the source. It contains three different functional groups: $-COO^-$ (carboxylate), –C–O–C– (ether) and –OH (alcohol). According to Nava Soucedo [20] and Velings [8], the nature of the alginate depends on the M/G ratio of alginate and also the polymer (alginate) and metal

salt's initial concentrations has an effect on the structure and properties of the final metal alginate synthesis.

The proportion of M and G residues and their macromolecular conformation determine the physical properties and the affinity of the alginate for divalent metal ions [21]. Alginates are able to adopt an ordered solution conformation through dimerization of the poly-G sequences in the presence of Ca^{2+} or other divalent cations, and this description is known as the "egg-box" model [22]. According to Grant et al. [23], the egg-box model is generally invoked to explain how the divalent metal ions, bounded in the interchain cavities, essentially polyguluronate sequences, give rise to a rod-like cross-link complex [24].

The egg-box model, which is the association of polyguluronate sequences by chelation of metal ion, is proposed by Rees and Welsh [7]. Oxygen atoms coordinated to metal ion are shown as filled circle. When drops of sodium alginate solution get into a divalent metal chloride solution, beads are immediately formed. During the first few minutes, the beads stay on the top of the solution. After a while (depending on the type of cation) they sink into the solution due to an increase of the density. This period is known as the maturation step.

Alginate has been well known to form ionotropic hydrogels in the presence of divalent cations (exclusive of Mg^{2+}) which act as crosslinkers between the functional groups of alginate monomers [25–29]. The alginate contained carboxyl group in their structure that define the adsorption capacity for metal ions. The product is basically formed by one ion-exchange reaction. This product can be used in many sectors like heat and sound insulation, carrier for catalysis, to release entrapped biomolecules such as pesticides, drugs, preservative, etc. [30–35] and in environmental technologies as well as in the packaging sector instead of Styrofoam [36]. Environmental concerns are also playing an increasingly important role, contributing to the growing interest in natural polymers due to their biodegrability, low toxicity and low disposal costs. The usually low manufacture costs of biopolymers, related to their large agricultural availability and renewability, is an additional advantage. Furthermore, their versatility of chemical structure (due to the presence of functional group like –C–O–C, –COO and –OH) and the chemistry of interaction of metal ion is well known which allow the development of advanced functionalized materials that can match several varied requirements.

The main objective of our study is to prepare alginic acid and metal alginates from fresh algae and their comparative study using different techniques such as Fourier transform infrared spectroscopy (FTIR), differential scanning calorimetry (DSC), scanning electron microscopy (SEM), porosity and thermogravimetric analysis (TGA).

Experimental

Materials Used

Dried algae [Undaria pinnatifida (Sea mustard), a kind of brown seaweeds, Average molecular weight; 320 kDa, determined by viscometric methods, M/G ratio; 2.1] were supplied from Kyungsung University, Busan, South Korea.

Preparation Procedure of Divalent Metal Alginate

The dried algae 2 g was stirred with an alkali solution 1.5 wt% (sodium carbonate) for about 2 h at 50–60 °C. Alginate dissolves as sodium alginate to give very thick slurry. Sodium alginate solution was added drop wise to metal chloride (MCl_2; M=Ca and Co) solution taken in a wide mouth glass jar to form divalent metal alginate beads. Almost circular beads were formed and the wet beads were taken out of solution and washed with distilled water thoroughly to remove excess metal chloride present with the beads. After washing, the beads were air dried.

Preparation of Alginic Acid

The sodium alginate extract was treated with dilute mineral acid, HCl at room temperature. A gelatinous precipitate of alginic acid forms which cannot be filtered; it simply blocks any filter medium. It can be removed from the liquid by flotation. Time taken to remove gelatinous alginic acid (11 g) from the liquid was 10 min. The gelatinous alginic acid contained almost 1.5% alginic acid with 98.5% of water.

FTIR Spectra of Alginic Acid and Metal Alginate

FTIR spectra were recorded on a Perkin Elmer Spectrometer (Perkin Elmer Ltd., Beaconsfield, BUCKS-HP9 2FX, UK. The spectra were collected from 2000 to 800 cm^{-1} range in the transmission mode with 4 cm^{-1} resolution over 40 scans.

Differential Scanning Calorimetry

DSC measurements were performed in a DSC-60, using sample mass of 2 mg in a covered aluminum sample holder with a central pin hole at heating rates of 5–10 °C min^{-1} under dynamic air and nitrogen atmospheres, and at the flow rate of 40 mL min^{-1} under atmospheric pressure.

Scanning Electron Microscopy

The surface properties of metal alginate were studied using SEM. Specimen preparation was performed as follows: the

dried sample was mounted on stubs and sputter-coated with gold. Micrographs were taken on a SEM instrument (Hitachi, S-4100).

Porosity

Pore size distribution, total pore volume and porosity were measured using auto pore IV 9500 V1.05 (Micromeritics Instrument Corporation, Norcross, GA, USA). Equilibration time (10 s) as well as filling pressure of mercury (1.33 psia) was used in this study.

Thermogravimetric Analysis

Thermal analyses of samples were recorded on a thermal analyzer (Universal V4.1D) system. TGA scans were done from 30 to 800 °C at different heating rate (5, 10 and 20 °C/min) in nitrogen and air atmospheres.

Results and Discussion

Kohn and Furda [37] proposed three main factors for understanding the binding of metal cations by these polyguluronates, viz (i) the geometry of ligand, (ii) the separation between unit charges on the chain and (iii) when chain-association is part of the binding process, the ease with which the polysaccharide chains can pack.

Alginate dissolves as sodium alginate to give very thick slurry. This slurry also contains the part of the seaweed that does not dissolve, mainly cellulose. This insoluble residue is removed from the solution by filtration. The loss of weight during drying was found to be 94.6%.

The loss of weight during drying was calculated using the following formula: % weight loss = $[(W_1–W_2)/W_1*100]$, where W_1 and W_2 are the weight of the bead before and after drying, respectively.

The wet alginate beads had smooth surface and circular shape, whereas dried beads had gained rough surface and distorted shape (visualization). Ionic bonding between carboxylate groups of the sodium alginate with Ca^{2+} or Co^{2+} ions results in the formation of mechanically stable networks.

Fourier Transform Infrared Spectroscopy

The stretching of C=O of protonated carboxylic group of alginic acid occurs at 1730 and 1609 cm^{-1}, respectively (Fig. 1). It is also observed that, when the proton was displaced by a monovalent ion (sodium), the peaks appeared at 1601 and 1432 cm^{-1}, respectively. These peaks were assigned for asymmetric and symmetric stretching vibration of free carboxyl group of sodium alginate [38]. In the FTIR spectrum of alginic acid, the peaks around 1030 cm^{-1} were attributed to the stretching of C–O–C.

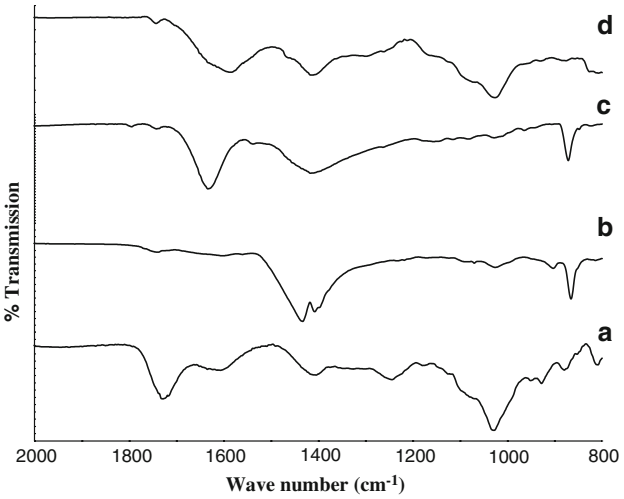

Fig. 1 FTIR spectra of (**a**) alginic acid, (**b**) sodium alginate, (**c**) calcium alginate, and (**d**) cobalt alginate

The peak at 1609 cm^{-1} for protonated carboxylic acid of alginic acid was shifted to the lower side due to the displacement of proton by divalent ion (calcium and cobalt) (Fig. 1). As divalent metal ions replaced sodium ions in the sodium alginate, the charge density, the radius and the atomic weight of the cation were changed, creating a new environment around the carbonyl group. Hence, a peak shifting should be expected.

Differential Scanning Calorimetry

The DSC curve of alginic acid, sodium alginate and calcium alginate at different heating rates (5 and 10 °C min^{-1}) under nitrogen and air atmospheres are presented in Fig. 2. In Fig. 2, DSC curve of alginic acid at different heating rates of 5 and 10 °C min^{-1} under nitrogen presented an endothermic peak around 18 and 31 °C (almost same at two heating rates), might be attributed to the dehydration process; whereas two small endothermic peaks around (158 and 162 °C) followed by a strong exothermic peak around (474 and 480 °C) have been seen which might be due to the decomposition of biopolymer. At the same time, DSC curve of alginic acid at different heating rates of 5 and 10 °C min^{-1} under air also shown an endothermic peak around (35 and 46 °C) due to the dehydration process taken place during heating, whereas small endothermic peaks around (163 and 170 °C), followed by a strong exothermic peak around (445 and 480 °C) might be attributed to the decomposition of biopolymer.

In the nitrogen atmosphere, an endothermic peak was shown around (102 and 100 °C) in the DSC curve of

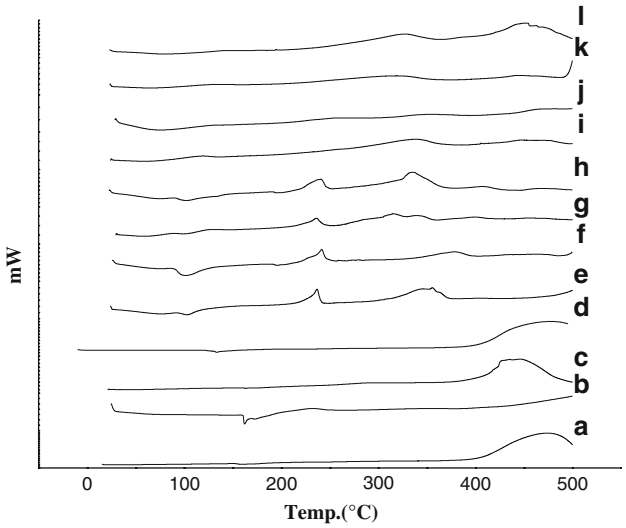

Fig. 2 DSC curve of [{alginic acid (**a**) heating rate = 5 °C/min, N_2 atmosphere (**b**) heating rate = 10 °C /min, N_2 atmosphere (**c**) heating rate = 5 °C/min, air atmosphere (**d**) heating rate = 10 °C/min, air atmosphere}, {sodium alginate (**e**) heating rate = 5 °C/min, N_2 atmosphere (**f**) heating rate = 10 °C /min, N_2 atmosphere (**g**) heating rate = 5 °C/min, air atmosphere (**h**) heating rate = 10 °C/min, air atmosphere} and {calcium alginate (**i**) heating rate = 5 °C/min, N_2 atmosphere (**j**) heating rate = 10 °C/min, N_2 atmosphere (**k**) heating rate = 5 °C/min, air atmosphere (**l**) heating rate = 10 C/min, air atmosphere}]

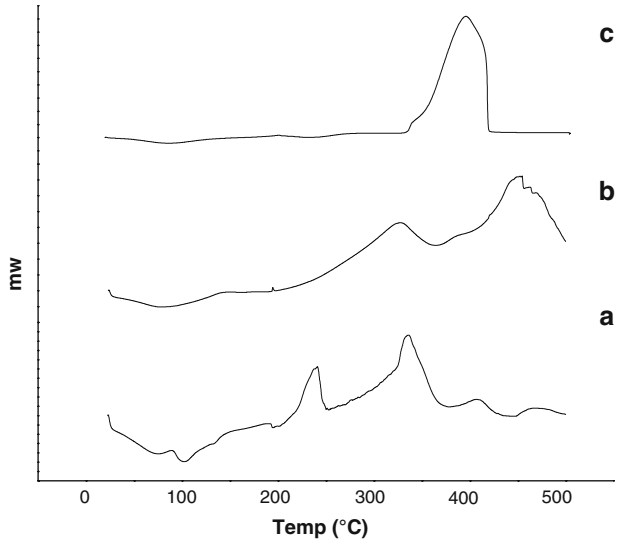

Fig. 3 DSC curve of (**a**) sodium alginate, (**b**) calcium alginate, and (**c**) cobalt alginate at heating rate = 10 °C/min in air atmosphere

sodium alginate at different heating rates (5 and 10 °C min^{-1}) might be due to the release of water (Fig. 2). On the other hand, exothermic peak with a maximum at (237 and 357 °C) and (240 and 382 °C) may be attributed to the biopolymer decomposition and formation of the respective carbonate [39]. But in air atmosphere an endothermic peak was presented around 100 °C, which may be attributed to the dehydration process whereas exothermic peaks occur with a maximum at (237 and 350 °C) and (240 °C and 335–407 °C). The decomposition process of biopolymer and formation of the respective carbonate might be responsible for these exothermic peaks.

In Fig. 2, DSC curve of calcium alginate at different heating rates of 5 and 10 °C min^{-1} under nitrogen presented an endothermic peak around (58 and 78 °C), could be attributed to the dehydration process whereas exothermic peak with a maximum at (337 and 448 °C) and (352 and 463 °C) might be responsible for the decomposition of biopolymer and formation of the respective carbonate. In presence of air at different heating rates of 5 and 10 °C min^{-1} also presented an endothermic peak around (65 and 78 °C), might be attributed to the water release, whereas exothermic peak with a maximum at (319 and 447 °C) and (327 and 453 °C) might be due to the decomposition of biopolymer and formation of the respective carbonate.

Figure 3 represents the DSC curve of sodium alginate, calcium alginate and cobalt alginate at heating rate (10 °C min^{-1}) in air atmosphere. The exothermic peak of sodium alginate occurred at 237 °C, whereas exothermic peak of calcium and cobalt alginate occurs at 327 and 396 °C, which might be due to the decomposition of biopolymer (Fig. 3). Thus, the decomposition of cobalt alginate occurs at higher temperature compared to sodium and calcium alginate; which could be concluded as the higher stability of cobalt alginate, in comparison to sodium and calcium alginate.

Scanning Electron Microscopy

SEM was employed to determine the surface properties of the metal alginate. The surface morphology of sodium alginate, calcium alginate and cobalt alginate at different magnifications are given in Fig. 4. SEM analysis revealed that surface morphology (at same magnification) changed with alteration of the metal ion. The difference in morphological structure formed with different metal cations can be explained by the different complexation mechanisms of these metal cations with alginates. Based on the SEM results, sodium alginate can be concluded as more porous compared to calcium and cobalt alginate; which tally with the porosity results.

Porosity

Porosity and pore structure are very important for the application of metal alginate in various fields. This analysis can give a wide variety of pore diameters varying from a few nano to several hundred nano meters. The total

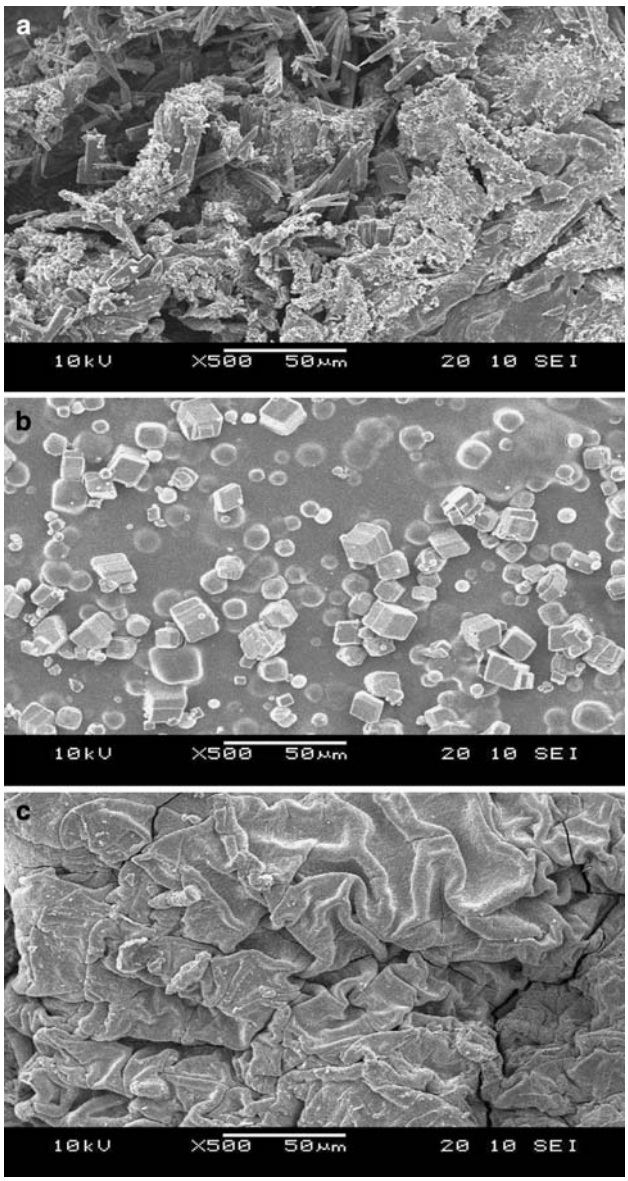

Fig. 4 Surface morphology of (**a**) sodium alginate, (**b**) calcium alginate, and (**c**) cobalt alginate at ×500 magnification

intrusion volume and porosity (%) of sodium, calcium, and cobalt alginates are shown in Table 1. It is observed in Table 1 that the total intrusion volume of sodium alginate (0.3787 mL/g) is much higher compared to those of calcium (0.0477 mL/g) and cobalt alginates (0.0970 mL/g). Similarly, porosity (%) of sodium alginate (56.8542) is much higher compared to those of calcium alginate (7.5143) and cobalt alginate (11.9708). When sodium ion in sodium alginate replaces by calcium or cobalt ion, the intrusion volume as well as porosity (%) of metal alginates is decreased. The results have shown that, the intrusion volume and porosity (%) of calcium alginate is lower compared to that of cobalt alginate. A plot of pore size

Table 1 Pore characteristic of sodium alginate

Sample	Total intrusion volume (mL/g)	Porosity (%)	Bulk density (g/mL)	Apparent density (g/mL)
Sodium alginate	0.3787	56.8542	1.5012	3.4793
Calcium alginate	0.0477	7.5143	1.5741	1.7020
Cobalt alginate	0.0970	11.9708	1.2347	1.4026

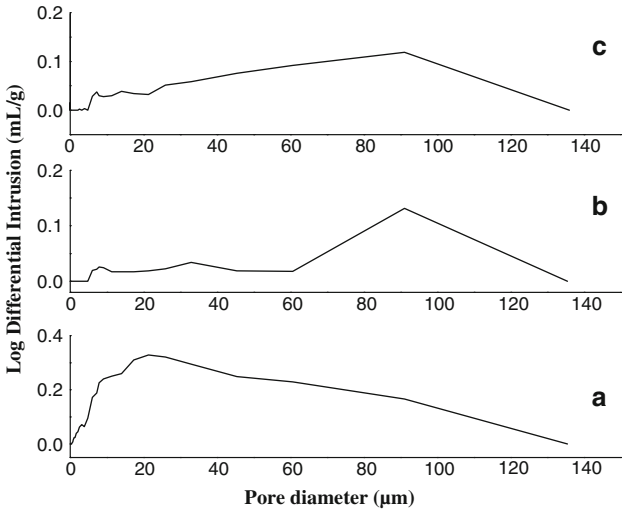

Fig. 5 Plot of pore size distribution of (**a**) sodium alginate, (**b**) calcium alginate, and (**c**) cobalt alginate

distribution (log differential intrusion) against pore diameter of sodium, calcium and cobalt alginate is given in Fig. 5. Sodium alginate showed broad pore size distribution; whereas narrow pore size distribution had been appeared in the case of calcium and cobalt alginate. Thus, it is concluded that pore size distribution of metal alginates is changed with presence of different metal ions.

Thermogravimetric Analysis

TGA is a very simple and accurate method for studying the degradation pattern and the thermal stability of polymers. The percentage weight loss values of various metal (Sodium, Calcium and Cobalt) alginate calculated from TGA data are listed in Tables 2–4. The results showed a stepwise weight loss during thermal sweep, indicating different types of reactions during degradation. It is seen from the tables that, all the alginates have started decomposing below 100 °C, but the rapid degradation were started at around 200 °C. Here, initial degradation may be attributed to the vaporization of moisture from the samples.

Table 2 Thermal analysis of sodium alginate in N_2 and air atmosphere

Nalg, N_2 atm				Nalg, air atm			
Temp. (°C)	% Weight loss (heating rate = 5 °C/min)	% Weight loss (heating rate = 10 °C/min)	% Weight loss (heating rate = 20 °C/min)	Temp. (°C)	% Weight loss (heating rate = 5 °C/min)	% Weight loss (heating rate = 10 °C/min)	% Weight loss (heating rate = 20 °C/min)
100	24.35	21.33	19.95	100	22.11	20.67	19.99
200	30.88	29.73	30.8	200	28.88	28.43	29.62
300	51.68	51.07	52.72	300	49.81	49.20	51.90
400	56.15	54.55	56.88	400	53.92	53.65	57.71
500	59.94	58.53	61.25	500	56.88	56.42	60.35
600	61.05	59.43	62.15	600	64.97	64.10	68.52
700	67.05	63.06	64.33	700	65.39	64.60	69.44
800	69.25	68.07	68.39	800	65.77	64.75	69.72

Table 3 Thermal analysis of calcium alginate in N_2 and air atmosphere

Calg, N_2 atm				Calg, air atm			
Temp. (°C)	% Weight loss (heating rate = 5 °C/min)	% Weight loss (heating rate = 10 °C/min)	% Weight loss (heating rate = 20 °C/min)	Temp. (°C)	% Weight loss (heating rate = 5 °C/min)	% Weight loss (heating rate = 10 °C/min)	% Weight loss (heating rate = 20 °C/min)
100	14.27	14.08	12.46	100	19.02	18.67	14.8
200	21.55	20.05	18.46	200	26.74	26.31	20.37
300	45.49	45.10	44.50	300	49.93	50.48	35.96
400	51.36	51.46	51.71	400	55.45	56.77	41.89
500	56.58	56.97	57.42	500	64.04	62.70	45.94
600	57.99	58.56	59.66	600	74.25	74.89	54.60
700	66.08	62.63	61.86	700	85.77	87.78	63.70
800	78.80	74.74	69.99	800	86.95	89.04	73.97

Table 4 Thermal analysis of cobalt alginate in N_2 and air atmosphere

Colg, N_2 atm				Colg, air atm			
Temp. (°C)	% Weight loss (heating rate = 5 °C/min)	% Weight loss (heating rate = 10 °C/min)	% Weight loss (heating rate = 20 °C/min)	Temp. (°C)	% Weight loss (heating rate = 5 °C/min)	% Weight loss (heating rate = 10 °C/min)	% Weight loss (heating rate = 20 °C/min)
100	14.33	12.11	11.45	100	16.64	16.89	11.45
200	22.36	20.27	22.71	200	25.82	25.13	22.71
300	40.44	39.23	50.47	300	52.91	48.41	50.47
400	54.74	52.65	66.72	400	67.89	66.39	66.72
500	71.03	68.31	66.82	500	68.05	66.53	66.82
600	78.00	73.97	66.87	600	68.22	66.59	66.87
700	78.59	78.04	66.93	700	68.31	66.66	66.93
800	78.94	78.41	67.09	800	68.40	66.69	67.09

The weight loss during 200–300 °C is most rapid and fast, which is corresponding to the biopolymer degradation [39]. The average percentage weight loss value at 300 °C in nitrogen atmosphere is comparatively higher for sodium alginates than those of calcium and cobalt compounds. All the alginates showed slow but steady degradation after 300 °C, but the degradation trends are different from one alginate to another. Thus, around 300 °C temperature, cobalt alginate is more stable comparing to those of sodium and calcium. At final temperature, the residue is containing mainly corresponding metal carbonate and also metal oxide [39].

Zohuriaan and Shokrolahi [39] reported the thermal study of sodium alginate. They showed that percentage weight loss is 37.1% in the temperature range 212.1–277.2 °C. But in the present case, the percentage weight loss for sodium alginate has reached the value of 50% at 300 °C.

Conclusions

Alginic acid was prepared from fresh algae using extraction method. Alginic acid converted into the metal alginate is confirmed by FTIR spectroscopy. The asymmetric stretching of free carboxyl group of calcium alginate occurred at 1630 cm^{-1} whereas asymmetric stretching of free carboxyl group of cobalt alginate appeared at 1585 cm^{-1}. DSC study reveals the shifting of peak positions on the curves with raising the heating rate. We can also conclude from DSC study that the decomposition of cobalt alginate has taken place at higher temperature in comparing to those of sodium and calcium alginate, which may be resulted into the higher stability of cobalt alginate. It is seen from SEM analysis that, surface morphology of metal alginates at same magnification alters with changing the metal ion. Sodium alginate is more porous compared to calcium and cobalt alginate. Pore size distribution of the alginates is also effected with the presence of various metal ions. At the same time, different metal alginates exhibit different thermal behavior due to the structural difference.

Acknowledgment Financial support from KIMST (2007) is duly acknowledged.

References

1. Sherrington DC (1977) In: Dyer A, Hudson MJ, Williams PA (eds) Progress in ion exchange: advances and application. The Royal Society of Chemistry, Cambridge, UK, pp 3–15
2. Rifi EH, Rastegar F, Brunette JP (1995) Talanta 42(6):811–816
3. Marsh SF, Svitra ZV, Bowen SM (1995) J Radioanal Nucl Chem 194(1):117–131
4. Muzzarelli RAA (1973) Natural chelating polymers. International series of monographs in analytical chemistry. Pergamon Press, Oxford, UK
5. Konishi Y, Asai S, Midoh Y, Oku M (1993) Sep Sci Technol 28(9):1691–1702
6. Mimura H, Ohta H, Akiba K, Onodera Y (2001) J Radioanal Nucl Chem 247(1):33–38
7. Rees DA, Welsh EJ (1977) Angew Chem Int Ed Engl 16(4):214–224
8. Velings NM, Mestdagh MM (1995) Polym Gels Netw 3:311
9. Kuyucak N, Volesky B (1989) Biotechnol Bioeng 33(7):823–831
10. Jang LK, Geesey GG, Lopez SL, Eastman SL, Wichlacz PL (1990) Chem Eng Commun 94:63–77
11. Jang LK, Lopez SL, Eastmen SL, Pryfogel P (1991) Biotechnol Bioeng 37(3):266–273
12. Strand KA, Boe A, Dalberg PS, Sikkeland T, Smidsrod O (1982) Macromolecules 15:570–579
13. Timmins P, Delargy P, Minchom CM, Howard R (1992) Eur J Pharm Biopharm 38:113–118
14. Aslani P, Kennedy RA (1996) J Control Release 42:75–82
15. Sabra W, Deckwer WD (2005) In: Dumitriu S (ed) Polysaccharides 'structural diversity and functional versatility'. Marcel Dekker, New York, p 515
16. Stanford P, Baird J (1983) The polysaccharides. Academic Press, New York
17. Wang ZY, Zhang QZ, Konno M, Saito S (1991) Chem Phys Lett 186:463
18. Chanda SK, Hirst EL, Percival BGV, Ross AG (1952) J Chem Soc 1833–1837
19. Chan LW, Lee HY, Heng PWS (2002) J Pharm 242:259
20. Nava Saucedo JE, Audras B, Jan S, Bazinet SE, Barbotin JN (1994) FEMS Microbiol Rev 14:93
21. Zheng H (1997) Carbohydr Res 302(1–2):97–101
22. Morris ER, Rees DA, Thom D, Boyd J (1978) Carbohydr Res 66(1):145–154
23. Grant G, Morris E, Rees D, Smith P, Thom D (1973) FEBS Lett 32:195
24. Yokoyama F, Achife C, Takakira K, Yamashita Y, Monebe K (1992) J Macromol Sci Phys B 31:463
25. Smidsrod O (1974) Faraday Discuss Chem Soc 57:263–274
26. Grasdalen H, Larsen B, Smidsrod O (1979) Carbohydr Res 68:23–31
27. Grasdalen H, Larsen B, Smidsrod O (1981) Carbohydr Res 89(2):179–191
28. Ouwerx C, Velings N, Mestdagh N, Axelos MAV (1998) Polym Gels Netw 6(5):393–408
29. Bajpai SK, Sharma S (2004) React Funct Polym 59(2):129–140
30. Martinsen A, Storro I, Skjak-Break G (1992) Biotechnol Bioeng 39:186
31. Estape D, Godia F, Sola C (1992) Enzyme Microb Technol 14:396
32. Andreopoulos A (1987) Biomaterials 8:397
33. Mehmetoglu U (1990) Enzyme Microb Technol 12:124
34. Hannoun B, Stephanopoulos G (1986) Biotechnol Bioeng 28:829
35. Longo M, Novella I, Garcia L, Diaz M (1992) Enzyme Microb Technol 14:586
36. http://www.nature.com/news/2002/021014/full/news021014-4.html
37. Kohn R, Furda I (1968) Collect Czech Chem Commun 33:2217
38. Kim SJ, Yoon SG, Kim SI (2004) J Appl Polym Sci 91:3705
39. Zohuriaan MJ, Shokrolahi F (2004) Polym Test 23:575